AISC Provisions for Web Stability Under Local Compression Applied to HSS

FEI WEI and JEFFREY A. PACKER

ABSTRACT

The relevant limit states for local compression loading on the webs of a rectangular HSS member are reviewed, and the 2016 AISC *Specification* Chapter J provisions are adapted from their normal application to the single web of a W-shape or I-section to this case. Two recent laboratory tests on matched-width, rectangular HSS-to-HSS cross-connections are described to illustrate the behavior of such connections under branch axial compression. The data from these tests are supplemented by experimental results from a further 76 cross-connection tests, with the branches being either welded plates or welded HSS. From this 78-test database, the existing provisions for local yielding of the chord sidewalls, local crippling of the chord sidewalls, and buckling of the chord sidewalls are evaluated. Recommendations are made for handling transverse compression loading on HSS webs in the AISC *Specification*, and a design example is given to illustrate the approach.

KEYWORDS: hollow structural sections, cross-connections, web yielding, web crippling, web buckling, design procedures.

INTRODUCTION

Concentrated compression forces on rectangular HSS are relatively common, especially at bearing or reaction points of trusses and girders and at beam-to-column moment connections. This loading situation is covered in AISC *Specification* Section K2.3 (AISC, 2016), where one is directed to determine the connection available strength from the applicable limit states in Chapter J.

For loading across the full width of the HSS (or when the branch-to-chord width ratio $\beta = 1.0$), the two webs are loaded in compression, and yielding or instability of the chord/column webs will control the connection capacity. AISC *Specification* Section J10 (AISC, 2016) on "Flanges and Webs with Concentrated Forces," which is based on the behavior of I-shaped sections with a single web, specifies the applicable limit states. For laterally supported HSS connections these are (1) web local yielding (Section J10.2), (2) web local crippling (Section J10.3), and (3) web compression buckling (Section J10.5). In the following, these limit states are further described, applied to the case of HSS webs, and evaluated against test results for matched-width, HSS-to-HSS cross-connections and plate-to-HSS connections under transverse compression. For all three limit states, the AISC *Specification* considers separate cases of the concentrated compression load being applied: (1) away from the member end (termed "interior" herein) and being free of any end effects and (2) close to the member end (termed "end" herein). The latter would correspond to a compression load close to an open end of an HSS member, without a cap plate. This paper evaluates transversely loaded HSS connections remote from the member end.

Fei Wei, Structural Engineer, Cast Connex Corporation, Toronto, Ontario, Canada. E-mail: fei.wei@mail.utoronto.ca

Jeffrey A. Packer, Bahen/Tanenbaum Professor of Civil Engineering, Department of Civil & Mineral Engineering, University of Toronto, Toronto, Ontario, Canada. E-mail: jeffrey.packer@utoronto.ca (corresponding)

Paper No. 2019-11R

Web Local Yielding

Local yielding of the HSS webs is a possible limit state for both compression and tension concentrated loads, and it applies to T-, Y- and cross- (or X-) connections with $\beta \approx 1.0$. The applied load, acting over a bearing length of l_b, disperses at a slope of 2.5:1 to the "k line" and thus produces yielding over a length of $(5k + l_b)$ for an interior connection. This load-dispersion angle of 21.8° is a classical assumption throughout steel codes. The distance k, from the outer face of the flange to the web toe of the fillet for a wide flange or I-section, can be taken for a rectangular HSS as the outside corner radius, with a conservative value of $1.5t$, where t is the HSS member design thickness (AISC *Specification* Section J10 Commentary). The applicable connection nominal strength equations, in both wide-flange (or I-section) format and HSS format, are shown in Table 1 for interior- and end-loading situations. In laboratory experiments, this failure mode has been found to occur for short bearing lengths (such as with plate-to-HSS connections, as shown in Figure 1) and also for stocky chord walls with longer bearing lengths.

Web Local Crippling

This limit state is defined as the crumpling of the web into buckled waves directly beneath a compression load, occurring in more slender webs, whereas web local yielding of that same area occurs for stockier webs (AISC *Specification* Section J10.3 Commentary). Research by Roberts (1981) on the compression of a single, slender, I-section web provided the basis for the nominal strength expressions in the AISC *Specification*. As shown in Table 1, modified versions are provided for interior- and end-loading situations. Because the overall member depth, d, is used in the I-section web crippling AISC *Specification* Equation J10-4, for consistency this is replaced by the HSS overall depth, H, in the conversion shown in Table 1. This is a small and conservative difference to the presentation in the 2010 AISC *Specification* Equation K2-10 (AISC, 2010). This limit state is applicable to "compressive single-concentrated forces" (*Specification* Section J10.3), hence to T- and Y-connections with $\beta \approx 1.0$. However, this failure mode has not been observed in rectangular HSS connections, which is presumed to be because the typical H/t values of HSS webs are below the wall slenderness requirement for this failure mode to govern. [Note that the tests reported by Roberts (1981) had overall height-to-web thickness ratios ranging from 75 to 505, with very few below 100.] Nevertheless, although the scope of the study presented herein is for HSS cross-connections, the applicable connection nominal strength equations for web local crippling, in both wide flange (or I-section) format and HSS format, are shown in Table 1.

Web Compression Buckling

This limit state involves overall buckling of the entire web and only applies to "a pair of compressive single-concentrated forces" (AISC *Specification* Section J10.5), hence to HSS cross-connections with $\beta \approx 1.0$, where compression force is transferred through the chord/column member. AISC *Specification* Section J10.5 Commentary notes that the nominal strength expression (for W- or I-shapes) is only valid for bearing lengths "…for which l_b/d is approximately less than 1." A validity range of l_b/d is hence included in Table 1. AISC *Specification* Equation J10-8 originates from Newlin and Chen (1971), who showed that their semi-empirical expression was a lower bound for web buckling failure loads achieved in a small number of transverse compression tests on point-loaded, wide-flange sections. AISC *Specification* Section J10 Commentary points out that *Specification* Equation J10-8 assumes pinned restraints at the ends of the web.

The dimension h is defined as the clear distance between flanges less the fillet or inside corner radius. Thus, in the conversion of web compression buckling formulas to HSS format, h is taken equal to $(H - 3t)$, which represents a maximum height of the flat part of the chord sidewall. For long bearing lengths, greater than the HSS overall depth, H, the web needs to be designed as a column member in accordance with AISC *Specification* Chapter E. Treating each HSS web as a column with a rectangular cross section is actually the method for handling web compression failure in Eurocode 3 (CEN, 2005), CIDECT Design Guide No. 3 (Packer et al., 2009), and ISO 14346 (ISO, 2013). This failure mode has been observed experimentally for full-width HSS-to-HSS cross-connections with H/t greater than about 15 (Figure 2). An earlier investigation on the influential parameters affecting the web strength of HSS chords under transverse compression, by Davies and Packer (1987), indicated that the bearing length parameter, l_b/H, affects the chord sidewall slenderness, H/t, at which failure changes from web bearing (local yielding) to web buckling.

For web compression buckling with $l_b > d$, or $H_b/\sin\theta > H$ (i.e., beyond the applicable limit of Table 1), each web is to be treated as a column of slenderness KL/r, where the effective length factor, K, can be taken as 1.0 (as suggested by AISC *Specification* Appendix Section 7.2.3, considering the main HSS through member as a non-sway frame). The column length, L, is taken as the sidewall flat dimension, equal to $(H - 3t)$. The radius of gyration, r, of a rectangular cross-section HSS wall is $t/\sqrt{12}$. Thus, the nominal

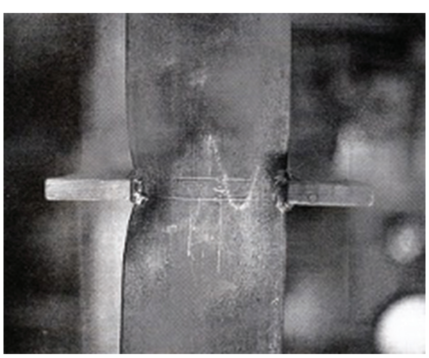

Fig. 1. Web local yielding failure in a full-width plate-to-HSS connection, with plates in compression.

Fig. 2. Web buckling failure in a full-width ($\beta = 1.0$) HSS-to-HSS cross-connection, with branches in compression and $H/t = 23$.

Table 1. Nominal (and Available) Strengths of Web Compression Limit States for Wide Flange (I-Section) Shapes and Rectangular HSS Connections, per the AISC *Specification* (Equation Numbers and ϕ/Ω Values from the *Specification*)			
Limit State	**Wide Flange or I-Section, R_n (kips)**	**HSS-to-HSS Connection, P_n (kips)**	**ϕ (Ω)**
Web local yielding, interior	for $l_{end} > d$ $F_{yw}t_w(5k + l_b)$ (J10-2)	for $l_{end} > H$ $\dfrac{2F_y t}{\sin\theta}\left(7.5t + \dfrac{H_b}{\sin\theta}\right)$ (1)	1.00 (1.50)
Web local yielding, end	for $l_{end} \le d$ $F_{yw}t_w(2.5k + l_b)$ (J10-3)	for $l_{end} \le H$ $\dfrac{2F_y t}{\sin\theta}\left(3.75t + \dfrac{H_b}{\sin\theta}\right)$ (2)	1.00 (1.50)
Web local crippling, interior	for $l_{end} \ge d/2$ $0.80t_w^2\left[1+3\left(\dfrac{l_b}{d}\right)\left(\dfrac{t_w}{t_f}\right)^{1.5}\right]\sqrt{\dfrac{EF_{yw}t_f}{t_w}}Q_f$ (J10-4)	for $l_{end} \ge H/2$ $\dfrac{1.6t^2}{\sin\theta}\left(1+\dfrac{\dfrac{3H_b}{\sin\theta}}{H}\right)\sqrt{EF_y}Q_f$ (3)	0.75 (2.00)
Web local crippling, end, and $l_b/d \le 0.2$	for $l_{end} < d/2$ $0.40t_w^2\left[1+3\left(\dfrac{l_b}{d}\right)\left(\dfrac{t_w}{t_f}\right)^{1.5}\right]\sqrt{\dfrac{EF_{yw}t_f}{t_w}}Q_f$ (J10-5a)	for $l_{end} < H/2$ and $H_b/H\sin\theta \le 0.2$ $\dfrac{0.8t^2}{\sin\theta}\left(1+\dfrac{\dfrac{4H_b}{\sin\theta}}{H}\right)\sqrt{EF_y}Q_f$ (4)	0.75 (2.00)
Web local crippling, end, and $l_b/d > 0.2$	for $l_{end} < d/2$ $0.40t_w^2\left[1+\left(4\dfrac{l_b}{d}-0.2\right)\left(\dfrac{t_w}{t_f}\right)^{1.5}\right]\sqrt{\dfrac{EF_{yw}t_f}{t_w}}Q_f$ (J10-5b)	for $l_{end} < H/2$ and $H_b/H\sin\theta > 0.2$ $\dfrac{0.8t^2}{\sin\theta}\left(0.8+\dfrac{\dfrac{4H_b}{\sin\theta}}{H}\right)\sqrt{EF_y}Q_f$ (5)	0.75 (2.00)
Web compression buckling, interior, and $l_b \le d$	for $l_{end} \ge d/2$ $\dfrac{24t_w^3\sqrt{EF_{yw}}}{h}Q_f$ (J10-8)	for $l_{end} \ge H/2$ and $H_b/H\sin\theta \le 1.0$ $\dfrac{1}{\sin\theta}\left(\dfrac{48t^3}{H-3t}\right)\sqrt{EF_y}Q_f$ (6)	0.90 (1.67)
Web compression buckling, end, and $l_b \le d$	for $l_{end} < d/2$ $\dfrac{12t_w^3\sqrt{EF_{yw}}}{h}Q_f$	for $l_{end} < H/2$ and $H_b/H\sin\theta \le 1.0$ $\dfrac{1}{\sin\theta}\left(\dfrac{24t^3}{H-3t}\right)\sqrt{EF_y}Q_f$ (7)	0.90 (1.67)
Note: l_{end} = distance from the near side of the connecting branch or plate to end of member			

flexural buckling strength of the two HSS sidewalls can be calculated from AISC *Specification* Section E3, with an allowance for an inclined branch producing a longer web buckling length (Packer et al., 2009; IIW, 2012; ISO, 2013) by:

$$\frac{KL}{r} = \frac{L_c}{r} = 3.46\left(\frac{H}{t} - 3\right)\sqrt{\frac{1}{\sin\theta}} \tag{8}$$

and, for one sidewall, a "column" cross-sectional area given by $A_g = (7.5t + H_b/\sin\theta)t$, from Equation 1 in Table 1 for $l_{end} > H$, or $A_g = (3.75t + H_b/\sin\theta)t$ from Equation 2 in Table 1 if $l_{end} \le H$. For consistency with Equations 6 and 7 in Table 1, the factor Q_f (from AISC *Specification* Table K3.2) should also be included if chord compression stress is present.

A recent numerical study of welded, full-width, rectangular HSS cross-connections by Kuhn et al. (2019) showed that 0.25 represented a critical value for the bearing length-to-chord height ratio at which the failure mode changed from web yielding to web buckling. Thus, for rectangular HSS-to-HSS cross-connections and plate-to-HSS cross-connections with $(H_b/\sin\theta)/H \le 0.25$, web local yielding was deemed to govern and could be predicted by a model such as Equation 1. H_b represents either the HSS branch depth, in the plane of the connection or, alternatively, the thickness of a transverse, full-width plate. If $(H_b/\sin\theta)/H > 0.25$, web compression buckling was deemed to govern and could be predicted by treating the two chord sidewalls as columns, for which a modification of Equation 1 could be used:

$$P_n = \frac{2\chi F_y t}{\sin\theta}\left(7.5t + \frac{H_b}{\sin\theta}\right) \tag{9}$$

where χ is a reduction factor applied to yield stress for column buckling. For fully welded branches to either side of the chord member, the end fixity of the sidewall "column" is likely closer to fixed-fixed than pin-ended. For fixed-fixed end conditions, Kuhn et al. (2019) noticed that most steel codes have a cold-formed column buckling curve that is almost linear when plotted over a practical chord sidewall slenderness range; hence they advocated a simple conservative estimation for χ using:

$$\chi = 1.15 - 0.013\frac{H}{t}\sqrt{\frac{1}{\sin\theta}} \le 1 \tag{10}$$

Equation 10, for $F_y \le 50$ ksi and $H/t \le 50$, is shown plotted in comparison to the 2016 AISC *Specification* column buckling curve in Figure 3. The vertical axis in this figure, χ, is equivalent to the AISC *Specification* buckling stress, F_{cr}, divided by the yield stress, F_y. An effective length factor of K = 0.65 is used as a design approximation to the theoretical fixed-fixed factor of K = 0.5. This approach advocated by Kuhn et al. (2019) is also evaluated against test data later in this paper, in addition to the current 2016 AISC *Specification* method.

EXPERIMENTS ON FULL-WIDTH RECTANGULAR HSS CROSS-CONNECTIONS

Two recent laboratory tests (Wei, 2019) on matched-width, rectangular HSS-to-HSS 90° cross-connections are described to illustrate the behavior under branch axial compression. These were tested to failure under displacement control, in quasi-static branch compression, as shown in Figure 4, using a 1,000-kip-capacity universal testing machine. As can be seen from Figure 4, the branch compression load was reacted by a steel plate, which was secured to the laboratory strong floor, and no lateral restraint was provided to the chord member. Displacement was captured at many points by a Metris K-610 3D Dynamic Laser Measuring System together with a linear variable differential transformer (LVDT). All members were made of cold-formed HSS to either ASTM A500 Grade B/C (ASTM, 2018) or CSA G40.20/G40.21 (CSA, 2013), and two chord sizes were used: HSS 8×8×¼ and HSS 8×8×⅜. A common branch size of HSS 8×4×½ was used, oriented such that $\beta = B_b/B = 1.0$ and $\eta = (H_b/\sin\theta)/B = 0.5$. The branch thickness was selected to be greater than that of the chord to be certain that local branch yielding would not occur before the chord webs failed. Measured geometric properties are given in Tables 2 and 3. Mechanical properties of the two chord members were determined by tensile tests on coupons cut from the flat regions where there was no weld seam. Average measured values (using three coupons from each HSS) are shown in Table 4.

In both connection tests, sidewall buckling was the observed failure mode, and the maximum load, P_a, was achieved prior to the 3%B connection ultimate deformation

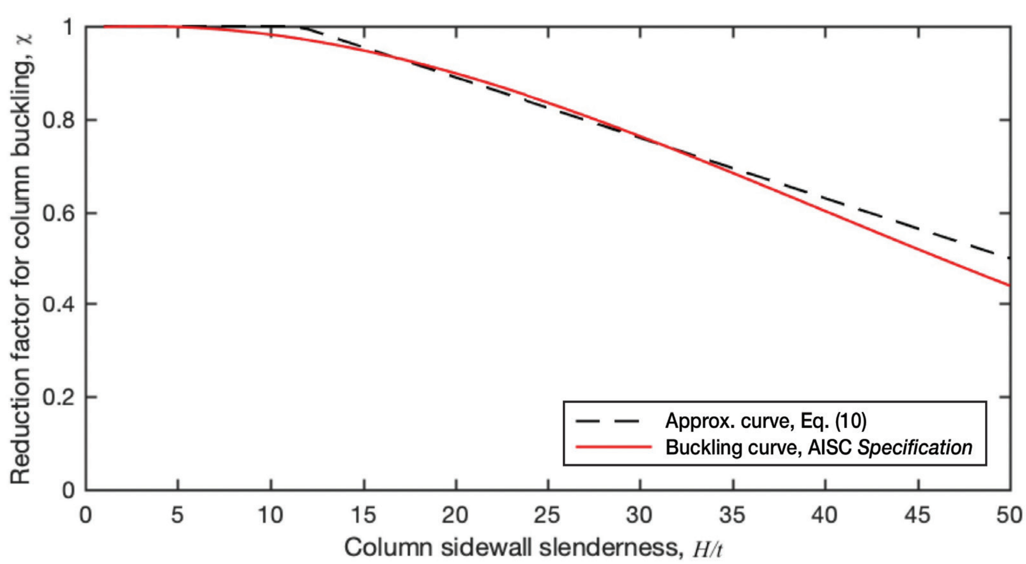

Fig. 3. AISC Specification *column buckling curve and the linear approximation of Equation 10, for* F_y = *50 ksi.*

Table 2. Test Specimens and Measured Geometric Variables						
Specimen	Width Ratio β	Chord Slenderness Ratio $2\gamma = B/t$	Wall-Thickness Ratio $\tau = t_b/t$	Chord Length (in.)	Branch Length (in.)	Fillet Weld Size (leg) (in.)
X1	1.0	34.7	2.17	41.4	20.0	0.25
X2	1.0	23.6	1.47	38.1	20.0	0.22

Table 3. Average Measured Rectangular HSS Cross-Sectional Dimensions					
Designation	Width B (in.)	Height H (in.)	Wall Thickness t (in.)	Corner Radius	
				Outer (in.)	Inner (in.)
HSS 8×8×¼	7.98	7.98	0.23	0.59	0.36
HSS 8×8×⅜	8.03	8.03	0.34	0.94	0.60
HSS 8×4×½	8.02	4.02	0.50	1.01	0.51

Table 4. Average Measured Rectangular HSS Chord Material Properties						
Designation	E (ksi)	F_y (ksi)	ε_y	F_u (ksi)	ε_{rup}	F_y/F_u
HSS 8×8×¼	30,180	57.1	0.0039	70.3	0.308	0.81
HSS 8×8×⅜	28,630	56.9	0.0040	71.6	0.334	0.79

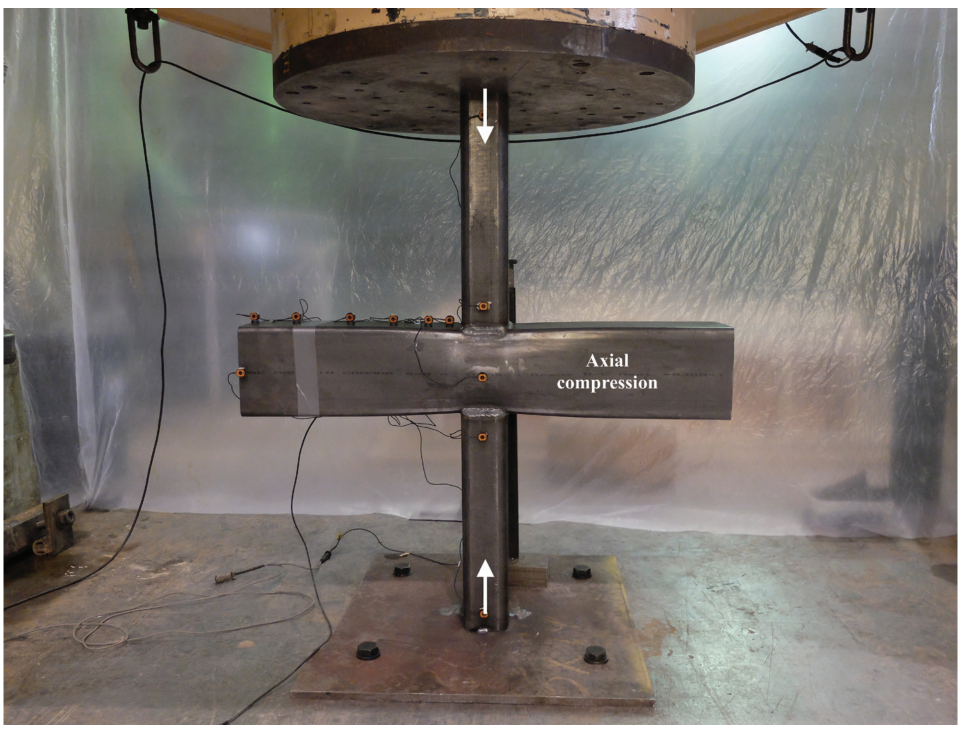

Fig. 4. Testing arrangement for rectangular HSS cross-connections, with failure by web buckling.

Table 5. Actual versus Predicted Ultimate Strengths and Failure Modes for Tests X1 and X2						
	Actual		Predicted			
Test No.	Ultimate Strength (kips)	Observed Failure Mode	Web Local Yielding Eq. (1)	Web Local Crippling Eq. (3)	Web Compression Buckling Eq. (6)	Web Compression Buckling Eqs. (10) and (14)
X1	**128**	Sidewall buckling	150.9	279.0	**105.2**	105.5
X2	**244**	Sidewall buckling	**254.2**	590.6	343.5	214.3

limit state (Lu et al., 1994). Thus, the connection ultimate strength was given by P_a, as shown on the load-displacement curves in Figure 5. To obtain the load-displacement curves in Figure 5, connection displacement was determined from the global vertical displacement of the difference between light-emitting-diode (LED) targets placed slightly above the chord face and the targets positioned at the centroid of the chord, and the branch compression load was provided by the testing machine's load cell. Table 5 compares the predicted ultimate strength and predicted failure mode, by the three limit states, with the observed strength and failure mode. For test X1, the capacity is reasonably predicted for the correct failure mode. For test X2, the capacity is reasonably predicted but for an incorrect failure mode. Both of these connections had a bearing length-to-chord height ratio of 0.50, but different H/t ratios (34.7 and 23.6). These results indicate that a wider review of these limit states—as applied to HSS connections—is warranted.

EVALUATION OF HSS WEB COMPRESSION LIMIT STATES

Although early design provisions have been evaluated (Packer, 1984, 1987), it is timely to apply the current 2016 AISC *Specification* rules to an expanded contemporary database of HSS experiments. Thus, aside from the two laboratory tests described, an additional 76 cross-connection tests from the literature were collated. This total database consists of 44 tests performed at the University of Toronto, 29 in the United Kingdom, and 5 in Spain. Pertinent data for all 78 tests is tabulated in Appendix G of Wei (2019). The group of 78 tests covers chord sidewall slenderness ratios (H/t) from 12.6 to 56.9; bearing lengths ranging from 0.07H to 3.72H; chord compressive stress up to 86% of chord yield stress; branch angles of 45°, 60°, and 90°; and three HSS production processes: cold-formed, cold-formed stress-relieved, and hot-formed. Measured geometric and

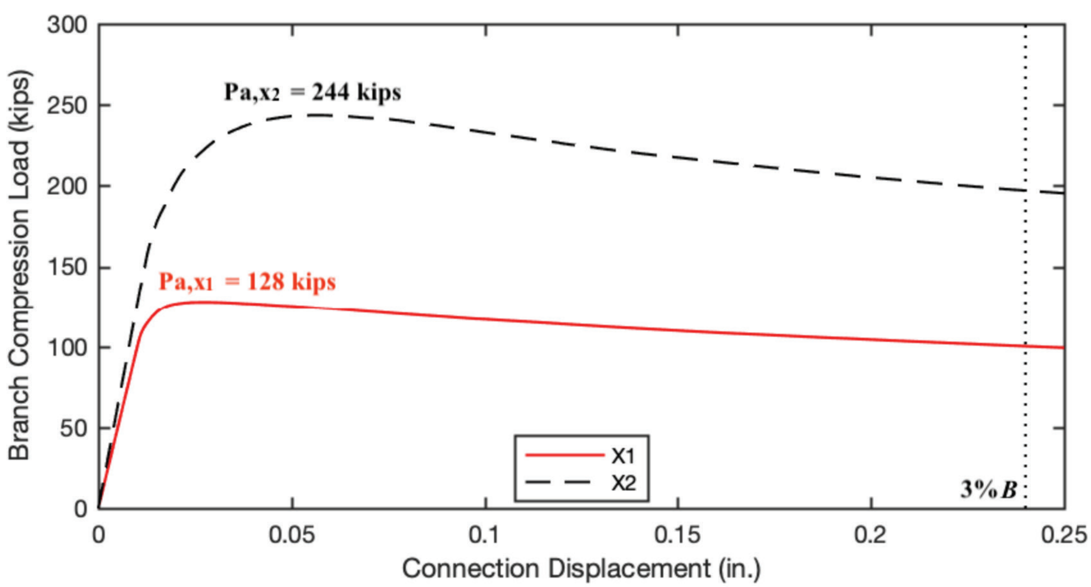

Fig. 5. Connection load-displacement curves for tests X1 and X2.

mechanical properties of the test specimens were used. Based on the configuration of individual connection tests, the database has been further divided into two categories: welded rectangular HSS to rectangular HSS connections and welded plate to rectangular HSS connections.

Welded Rectangular HSS to Rectangular HSS Connections

In this section, an evaluation is made of the current design provisions against 53 welded rectangular HSS to rectangular HSS cross-connections. When the bearing length of the load, $H_b/\sin\theta$, is less than or equal to the total depth of the chord member, H, the three web compression limit states (local yielding of the chord sidewalls, local crippling of the chord sidewalls, and buckling of the chord sidewalls) are represented by Equation 1, Equation 3, and Equation 6 respectively, as discussed earlier.

The correlation between actual experimental test results and predicted connection strengths is shown in Figure 6. Ultimate strengths P_n and P_a are used in the correlation plots, where P_n represents the connection theoretical capacity calculated from the limit states and P_a represents the actual experimental test results recorded by the researchers, both expressed as a force in the branch. Although the mean of this ratio is 1.37, the scatter is huge (COV = 0.45). A number of tests are overestimated, while some tests are significantly underestimated by the limit state of chord sidewall buckling. The large variability shown by chord sidewall buckling predictions indicates that the interior web compression buckling equation, Equation 6—when applied to rectangular HSS-to-HSS connections—is generally a poor predictor of the strength for this limit state. As noted earlier, Equation 6 originates from point-load tests on wide-flange section webs. In addition, none of the connection tests is governed by local crippling of the chord sidewalls, represented by Equation 3, indicating that this is not a viable failure mode over this range of data.

When the bearing length of the load is greater than the total depth of the chord member, each chord sidewall needs to be designed as a column with a slenderness ratio of KL/r. As discussed earlier, instead of using Equation 6, the nominal flexural buckling strength can be calculated using AISC *Specification* Section E3:

$$P_n = F_{cr} A_g \tag{11}$$

and the "column" cross-sectional area of one web can be calculated as:

$$A_g = \left(7.5t + \frac{H_b}{\sin\theta}\right)t \tag{12}$$

AISC *Specification* Section E3 applies the full gross cross-sectional area, A_g, to compression members with nonslender elements, as defined in Section B4.1; however, none of the cases included in Table B4.1a of the *Specification* directly correspond to a laterally compressed rectangular HSS sidewall. Hence, the full gross cross-sectional area, A_g, is always used in the sidewall buckling equation. The critical stress, F_{cr}, is determined based on the slenderness ratio of KL/r. The *Specification* and Commentary do not clearly state which value of the effective length factor, K, to use, and designers could adopt $K = 1.0$ to be conservative. Because $F_{cr} \le F_y$, the limit state of local yielding of the chord sidewalls is thus incorporated into the nominal flexural buckling strength by:

$$P_n = \frac{2F_{cr}t}{\sin\theta}\left(7.5t + \frac{H_b}{\sin\theta}\right)Q_f \tag{13}$$

where Q_f is a reduction factor to account for the effect of normal stress in the chord. All 16 connection tests with bearing length of the load greater than the total depth of the chord member were governed by the limit state of flexural buckling of the chord sidewalls, represented by Equation 13, and the correlation between actual experimental test results and predicted connection strengths, using $K = 1.0$, is shown in Figure 7.

With the two bearing length situations combined, correlation between the entire group of 53 welded rectangular HSS-to-HSS cross-connection tests is plotted in Figure 8. The mean ratio of actual/predicted capacity is 1.41 with a very large scatter (COV of 0.46). When the bearing length of the load is greater than the total depth of the chord member, web buckling failure predictions given by Equation 13 using $K = 1.0$ are conservative for a considerable number of the test results. In this case, 1 out of 53 tests had a ratio of actual/predicted capacity greater than 2.6, which did not fit into Figure 8(a). This correlation suggests that the end fixity of the sidewall "column" is more likely to be fixed-fixed rather than pin-ended for a chord member with branches welded to either side, which seems logical considering the large flare bevel groove welds at either end of the chord member web. This implies that the effective length factor, K, can better be taken as 0.65 instead of 1.0.

For these 53 welded rectangular HSS-to-HSS cross-connections, 42 of them have the failure mode recorded (although there may be misinterpretations of the initial failure mode by some researchers). Nine of the 42 connections had the failure mode incorrectly predicted when compared against the observed actual test failure mode (Wei, 2019). All nine of these incorrect predictions were a result of high predicted sidewall buckling strength.

Welded Plate to Rectangular HSS Connections

Unlike the welded rectangular HSS-to-HSS cross-connection tests, the load bearing length of all 25 welded plate to rectangular HSS cross-connection tests is less than the total

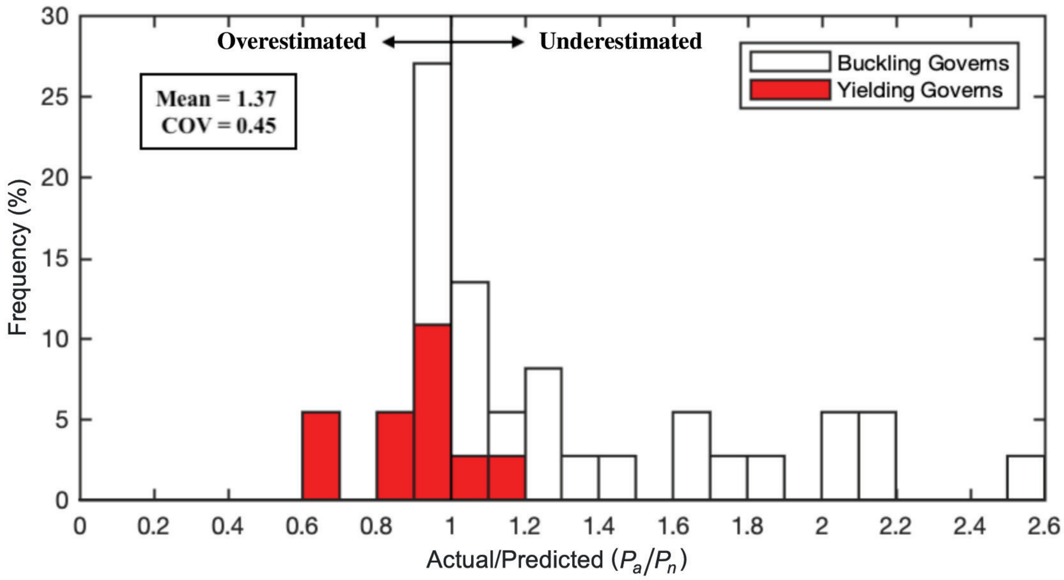

(a)

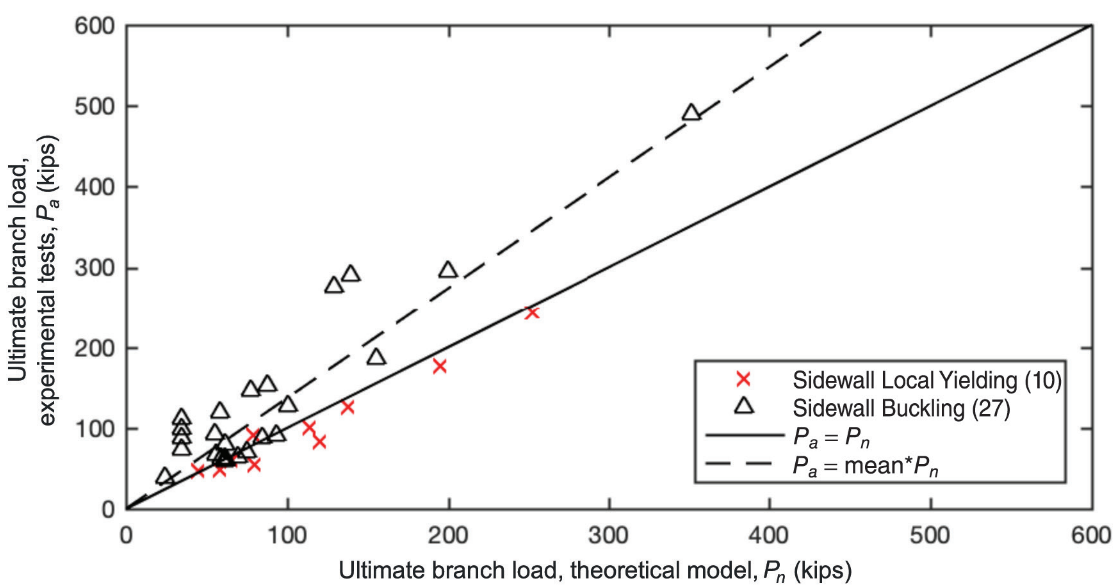

(b)

Fig. 6. Correlation between 37 welded rectangular HSS to rectangular HSS connection tests with bearing length ≤ H *and the 2016 AISC* Specification.

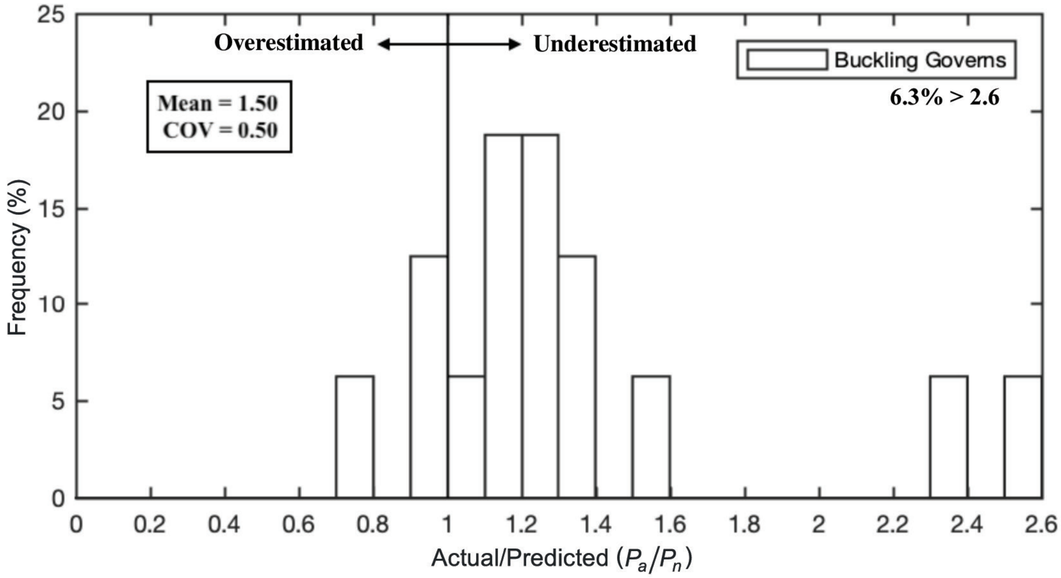

(a)

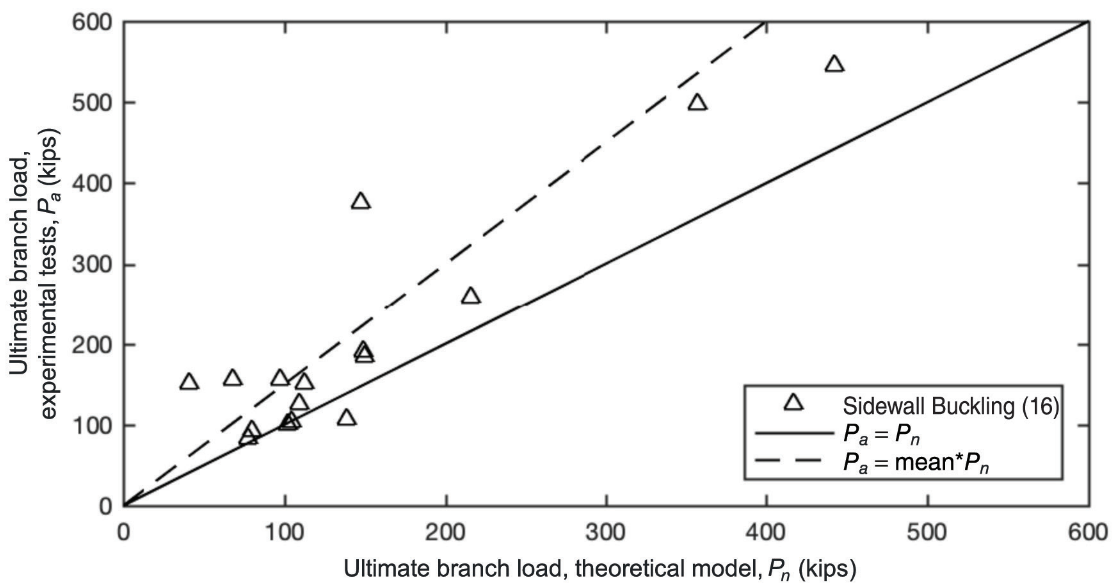

(b)

Fig. 7. Correlation between 16 welded rectangular HSS to rectangular HSS connection tests with bearing length > H *and 2016 AISC* Specification*, using* K = *1.0.*

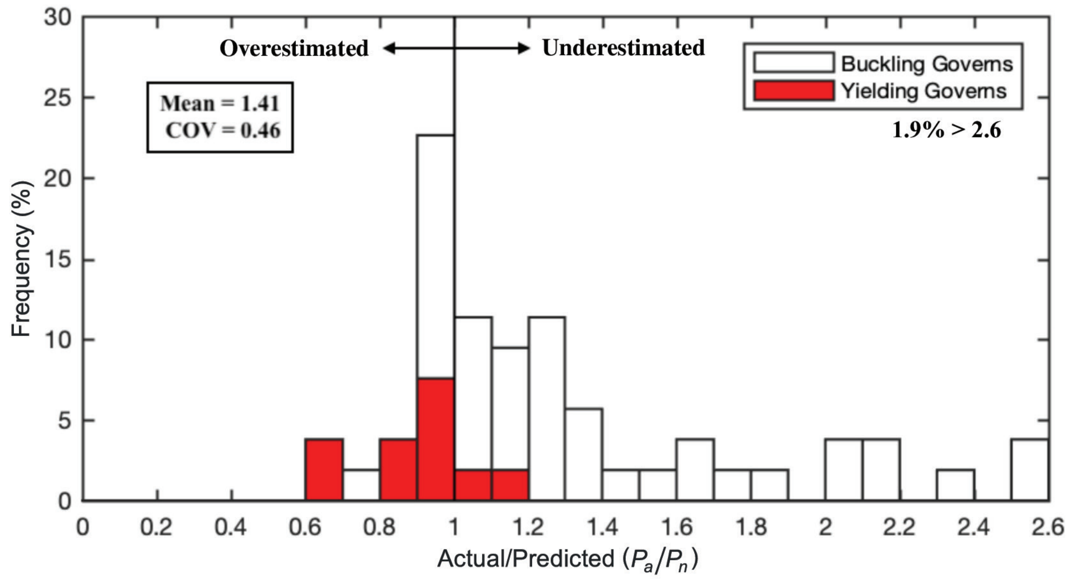

(a)

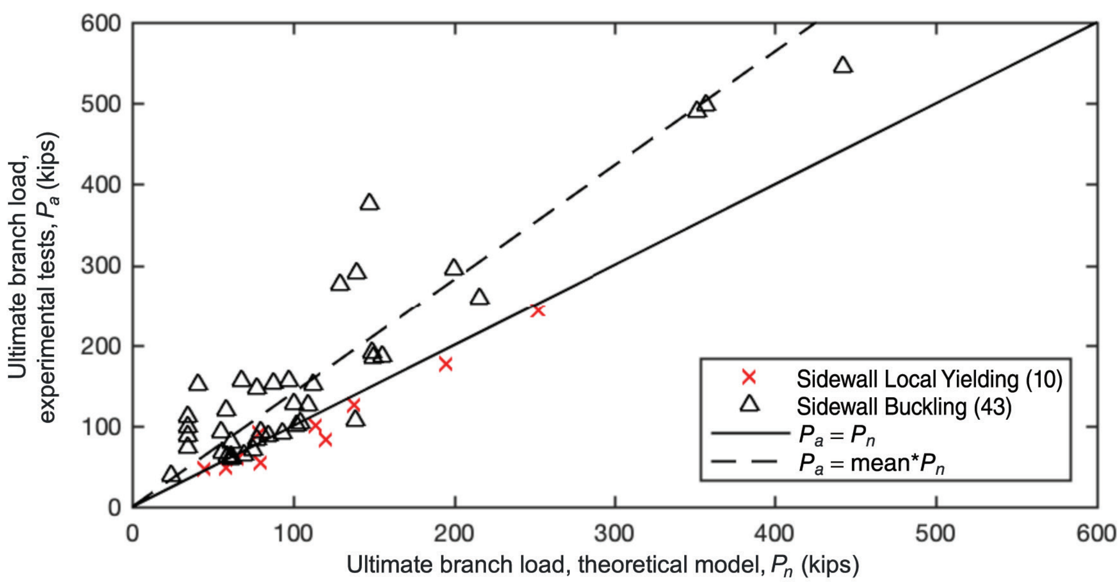

(b)

Fig. 8. Correlation between 53 welded rectangular HSS to rectangular HSS connection tests and the AISC Specification.

depth of the chord member. Thus, the web compression limit states are represented by Equation 1, Equation 3, and Equation 6. In this category, the web local yielding limit state governed the predicted strength of all cases, with only one exception. The actual-to-predicted strength distribution, shown in Figure 9(a), is much better compared to that of welded rectangular HSS-to-HSS connection tests. The mean is slightly greater than unity (1.15) with a relatively low spread of data, indicated by a COV of 0.18. Figure 9(b) shows a somewhat more conservative correlation by taking the predicted branch capacity as simply the vertical force component. These plots indicate the excellent applicability of the existing web local yielding model to HSS webs.

In Figure 9, the one test for which buckling governed had $H_b/H = 0.20$ and $H/t = 57$. Because $H_b/H < 0.25$, the breakpoint between web yielding and web buckling established by Kuhn et al. (2019), one might expect web yielding to govern. However, the 0.25 value was determined on the basis of numerical research on HSS up to $H/t = 50$ (Kuhn et al., 2019), so there may be less reliability in this breakpoint at $H/t > 50$. Nevertheless, in Figure 9 the actual strength far exceeds the predicted strength for this test and is conservative.

ALTERNATE MODELS

From the evaluation of existing test results for full-width, welded rectangular HSS cross-connections, it was shown that the 2016 AISC *Specification* web crippling equation and the web buckling equation, which are based on specific tests on I-section webs, either never govern or result in a large scatter in the predicted strengths when applied to the chord sidewall of rectangular HSS. One of the most influential parameters, bearing length $H_b/\sin\theta$, is absent from the web buckling equation. Even for connections where the strength prediction is governed by a sidewall flexural buckling equation, represented by Equation 13, the assumption of pinned-pinned end fixity ($K = 1.0$) leads to generally conservative estimates. Hence, the web compression limit states for rectangular HSS connections could be modified to one of the following.

Model 1

According to a recent numerical study by Kuhn et al. (2019), a failure mode transition from web local yielding to web buckling was observed at a critical bearing length $(H_b/\sin\theta) = 0.25H$. For bearing lengths greater than $0.25H$, the sidewall compression strength was well-predicted using the column flexural buckling approach, over a practical H/t range associated with manufactured HSS. Thus, the first proposed modification is to require HSS sidewalls to be considered as columns (and analyzed using AISC *Specification* Section E3) for bearing lengths greater than $0.25H$ [rather than the current $1.0H$, as indicated below Equation 6 in Table 1]. With this modification, the capacity of 37 welded rectangular HSS-to-HSS connections with bearing length $(H_b/\sin\theta)$ ranging from $0.25H$ to H, which are originally estimated as per Table 1, can now be predicted by Equation 13. A second proposed modification is to adopt an effective length factor of $K = 0.65$ instead of 1.0. Combined with the other 16 tests, the correlation between actual experimental test results and predicted connection strengths using Equation 13 is presented in Figure 10(a) to evaluate the effectiveness of these modifications.

A clear improvement can be observed by a comparison of Figure 10(a) with Figure 8(a). Although the COV of 0.27 is still not low, it is significantly reduced from the value of 0.46 obtained previously, which indicates that the sidewall flexural buckling equation, Equation 13, is a better strength predictor of connections with bearing length $(H_b/\sin\theta) > 0.25H$ when compared to web buckling Equation 6. Moreover, for connections with inclined branches (i.e., when $\theta < 90°$), there is a trend for the connection strengths to be overpredicted. Packer (1984) has already noted that the connection strength increase (measured as a force in the branch) is less than associated with $1/\sin\theta$. The effect of branch member inclination requires more study but, in the meantime, if one takes the predicted branch capacity as simply the vertical force component, the more-conservative correlation shown in Figure 10(b) is the result. In Figure 10, the connection capacity prediction is based on a column-buckling model, which incorporates both sidewall local yielding (squashing) and flexural buckling; hence, no legend (buckling governs/yielding governs) is given in this figure.

A simple reliability analysis (Fisher et al., 1978; Ravindra and Galambos, 1978) can be applied to the statistics (or model parameters) in Figure 10(b) in which a resistance factor, ϕ, is calculated using a target safety/reliability index of 3.0 and a coefficient of separation of 0.55. Furthermore, one can introduce statistical parameters to model geometric variations [as recommended by AISI (2016)] and typical material strength variations for ASTM A500 Grade B/C yield strength [as determined by Liu (2016)], the result of which is $\phi = 0.95$. Because a value of $\phi_c = 0.90$ is used in AISC *Specification* Section E1, which is lower, adequate safety/reliability is provided by Model 1 for welded rectangular HSS-to-HSS cross-connections.

For connections with a bearing length $(H_b/\sin\theta) \le 0.25H$ (all 25 welded plate to rectangular HSS connections), the capacity can be predicted by Equation 1 alone since the web local yielding limit state governed the predicted strength of all 25 cases, with only one exception. Applying this single limit state check to connections in this bearing length range leads to a mean value of 1.14 and a COV of 0.17, which are almost identical to what was obtained in Figure 9(a). If one takes the predicted branch capacity as simply the vertical

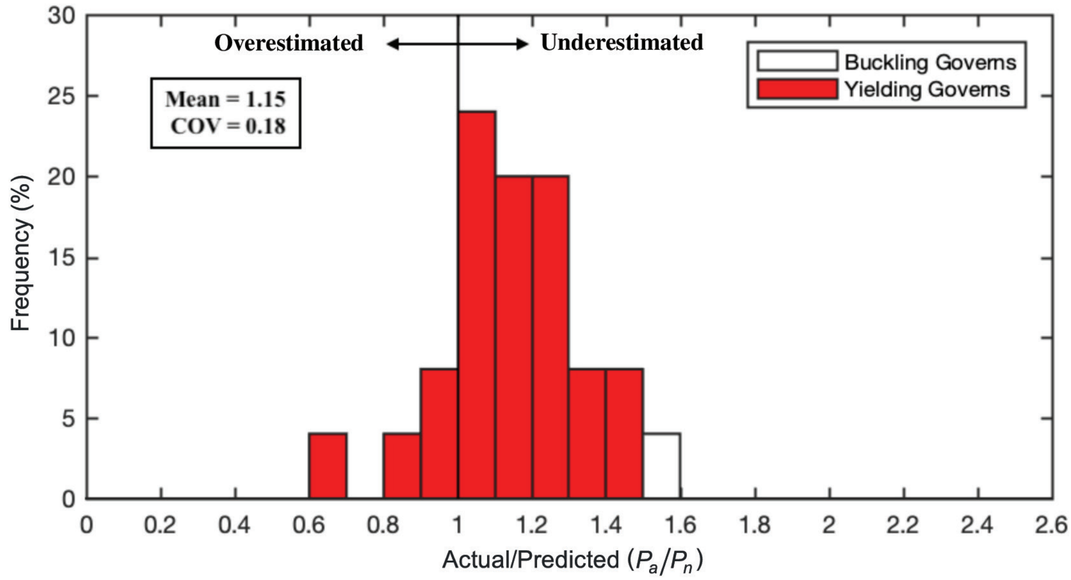

(a) Using Equation 1

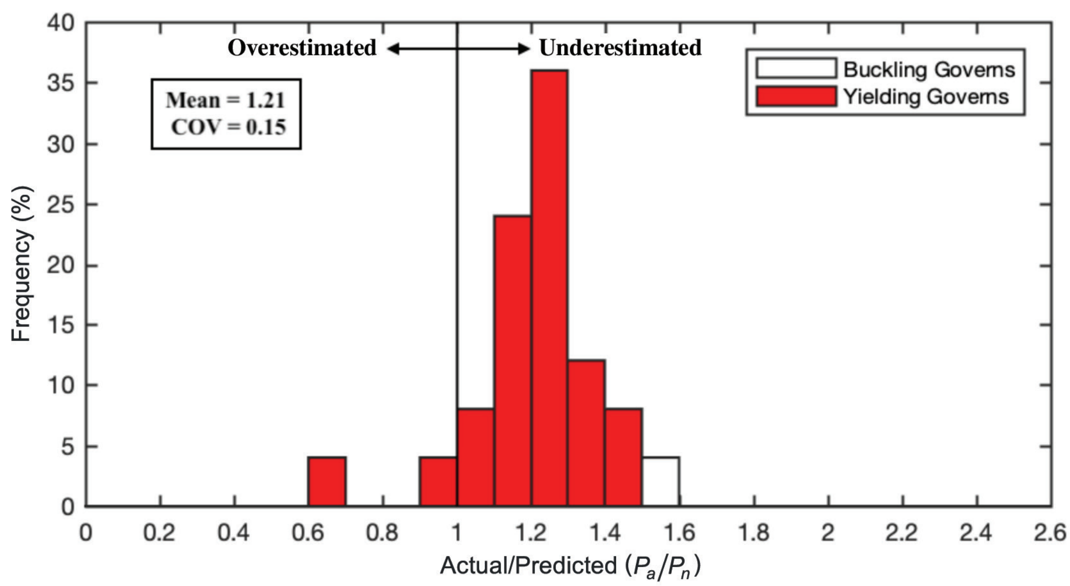

(b) Using Equation 1 but deleting the first sinθ term (below $2F_yt$*)*

Fig. 9. Correlation between 25 welded plate to rectangular HSS connection test and the 2016 AISC Specification.

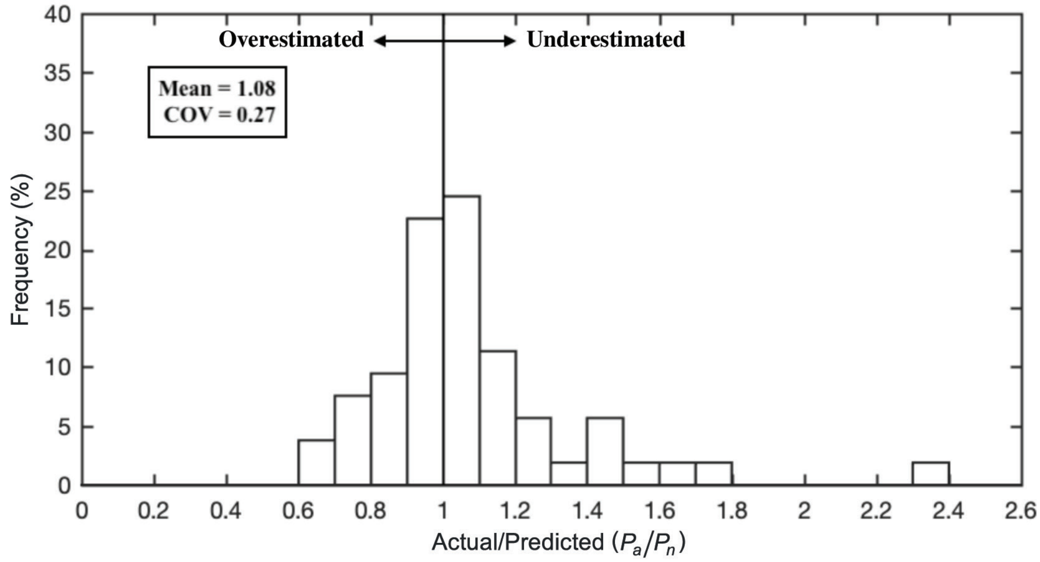

(a) Using Equation 13

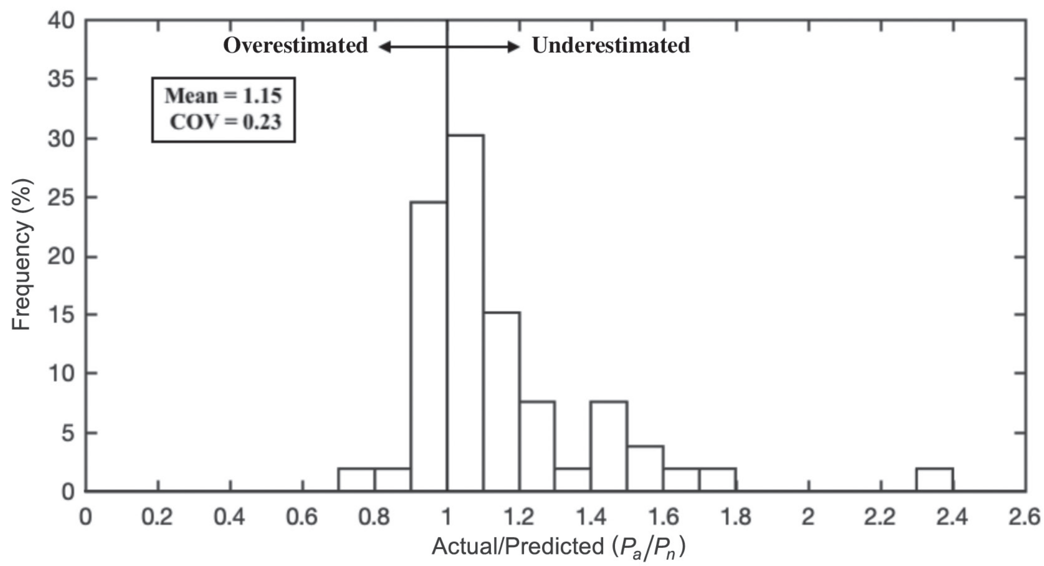

(b) Using Equation 13 but deleting the first sinθ term (below $2F_{cr}t$)

Fig. 10. Correlation between 53 welded rectangular HSS to rectangular HSS connection tests and Equation 13 with K = *0.65.*

force component a mean value of 1.19 and a COV of 0.15 result, which are almost identical to what was obtained in Figure 9(b). Performing the same reliability analysis as described above, but with model parameters of mean = 1.19 and COV = 0.15, one obtains $\phi = 1.09$. Because a value of $\phi = 1.00$ is used in AISC *Specification* Section J10.2, which is lower, adequate safety/reliability is provided by Model 1 for welded plate to rectangular HSS connections.

To design a full-width welded rectangular HSS-to-HSS cross-connection, the AISC *Specification* requires designers to check three web compression limit states: local yielding of the chord sidewalls, local crippling of the chord sidewalls, and buckling of the chord sidewalls. With this method, the predicted connection capacity can be based on either Equation 1 or Equation 13 with $K = 0.65$, depending on the connection bearing length. A recommended adjustment to these equations, for inclined branches with $\theta < 90°$, is to take the predicted branch capacity as the branch force vertical component. Maintaining the checks for all three limit states, but using the preceding recommendations, will still result in reliable predictions of connection capacity for the limit state that governs.

Model 2

Another simplified method to the foregoing is also possible. As discussed previously, Kuhn et al. (2019) advocated the use of Equation 10 for a reduction factor to be applied to yield stress for column buckling, χ, as it was noticed that most steel codes have a cold-formed column buckling curve that is almost linear when plotted over a practical chord sidewall slenderness range ($H/t \le 50$) for fixed-fixed end conditions. The AISC *Specification* buckling curve is no exception, as presented in Figure 3. Thus, to simplify the process of calculation, the critical stress, F_{cr}, can be replaced by χF_y to give a sidewall compression strength of:

$$P_n = \frac{2\chi F_y t}{\sin\theta}\left(7.5t + \frac{H_b}{\sin\theta}\right)Q_f \tag{14}$$

Of the 53 tests, 47 lie within the chord sidewall slenderness range of $H/t \le 50$. The correlation between actual experimental test results and predicted connection strengths using Equation 14 is shown in Figure 11(a) and, as expected, a similar relationship to Model 1 is obtained. The numerical research of Kuhn et al. (2019) was based only on 90° connections, so it would be logical to again investigate (as in Model 1) the correlation with experiments by taking the predicted branch capacity as simply the vertical force component. This results in the excellent correlation shown in Figure 11(b). In Figure 11, the connection capacity prediction is based on a single limit state model; hence, no legend (buckling governs/yielding governs) is given in this figure.

For welded plate to rectangular HSS connections or welded rectangular HSS-to-HSS connections with bearing length ($H_b/\sin\theta$) $\le 0.25H$, it is recommended for Model 2 that the buckling reduction factor, χ, be taken as 1.0. As connections within this range are very likely governed by sidewall local yielding, the correlation is again very similar to that shown in Figure 9.

CONCLUSIONS

AISC *Specification* Section J10 (AISC, 2016) provisions for concentrated compression forces on webs have been applied to the case of transversely compressed rectangular HSS members. These provisions have then been evaluated against 78 laboratory tests, taking the form of welded interior plate-to-HSS cross-connections and welded interior HSS-to-HSS cross-connections. The web local yielding limit state, represented by Equation 1 in Table 1, has been found to be very applicable to HSS. The web local crippling limit state, represented by Equation 3 in Table 1, has been found to never govern for the range of HSS examined (specified yield strengths up to 50 ksi and sidewall slenderness values up to 57). It has been shown that, for the web compression buckling limit state, represented by Equation 6 in Table 1, greater prediction accuracy can be obtained if a column buckling model is used when bearing lengths are greater than 0.25 of the chord depth. It is thus recommended (as a modification to AISC *Specification* Section J10.5 Commentary) that the HSS member web be designed as a compression member, in accordance with AISC *Specification* Chapter E, when l_b or ($H_b/\sin\theta$) > $0.25H$. Moreover, when doing so, the compression member (each web) can be taken to have a cross-sectional area given by Equation 12 and an effective length factor of $K = 0.65$. The influence of branch member inclination on connection capacity is not conclusive, so it is recommended that—in the case of inclined branches with $\theta < 90°$—one conservatively takes the predicted branch capacity, for all failure modes, as simply the vertical force component. Table 6, which can be compared to Table 1, provides a summary of the foregoing recommendations, applied to interior HSS connections. The limit state of web local crippling should be redundant for normal HSS sizes, but it is included in Table 6 for completeness and also in the design example that follows.

This review has studied connections that were not prone to out-of-plane stability. This will be the usual case when an HSS main member is subject to transverse compression because lateral restraint is generally provided (e.g., at reaction or load points of trusses and beam-to-column moment connections). It is conceivable that lateral instability of the chord member could arise with a lack of symmetry due to misalignment or with long compression-loaded branch members; in such cases, this should be incorporated in modeling structural behavior of the system.

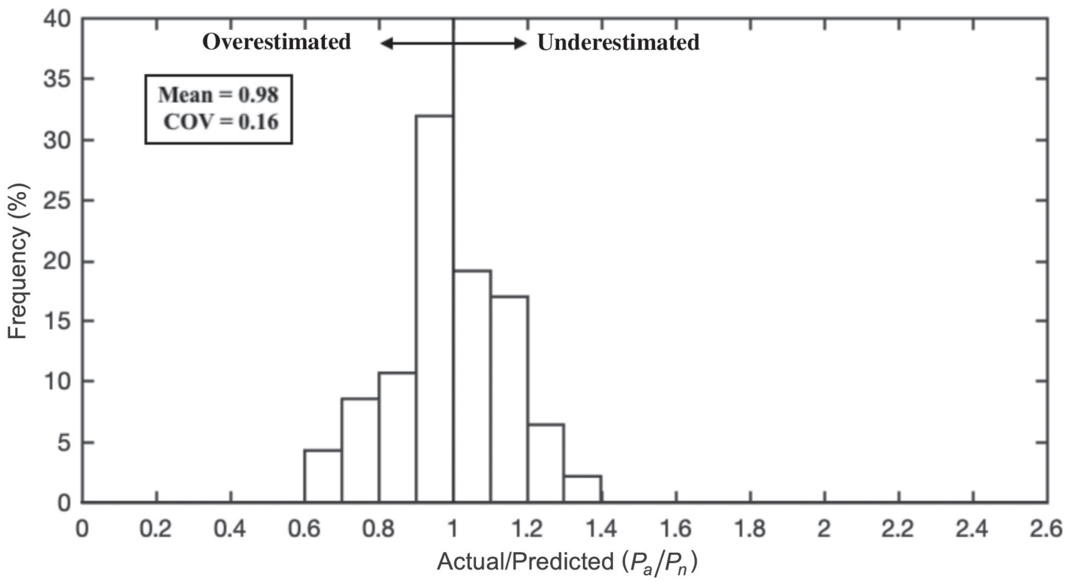

(a) Using Equation 14

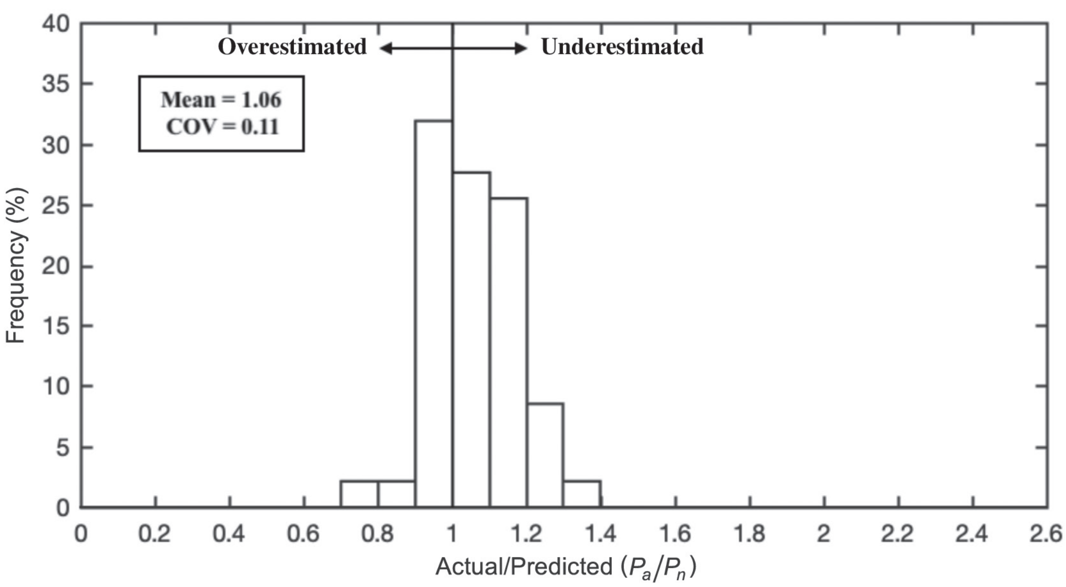

(b) Using Equation 14 but deleting the first sinθ *term (below* $2\chi F_y t$*)*

Fig. 11. Correlation between 47 welded rectangular HSS to rectangular HSS connection tests and Equation 14, with $H/t \leq 50$.

Table 6. Recommended Nominal (and Available) Strengths of Web Compression Limit States for Rectangular HSS Connections

Limit State	HSS-to-HSS Connection, P_n (kips)	ϕ (Ω)
Web local yielding, interior	for $l_{end} > H$ $2F_y t\left(7.5t + \dfrac{H_b}{\sin}\right)$ (15)	1.00 (1.50)
Web local crippling, interior	for $l_{end} \geq H/2$ $\dfrac{1.6t^2}{\sin\theta}\left(1+\dfrac{\frac{3H_b}{\sin\theta}}{H}\right)\sqrt{EF_y}Q_f$ (16)	0.75 (2.00)
Web compression buckling, interior, and $l_b \leq 0.25H$	for $l_{end} \geq H/2$ and $H_b/H\sin\theta \leq 0.25$ $\left(\dfrac{48t^3}{H-3t}\right)\sqrt{EF_y}Q_f$ (17)	0.90 (1.67)
Web compression buckling, interior, and $l_b > 0.25H$	for $l_{end} \geq H/2$ and $H_b/H\sin\theta > 0.25$ Use AISC *Specification* Equations E3-1, E3-2, and E3-3 with $K = 0.65$, L_c/r from Equation 8, and A_g (for each sidewall) from Equation 12	0.90 (1.67)

DESIGN EXAMPLE

Given:

Determine the adequacy of the welded rectangular HSS-to-HSS 90° cross-connection shown in Figure 12 subjected to the loads indicated. The branch members are oriented such that the chord is loaded across its full width, and the loads shown consist of 50% dead load and 50% live load. Assume the welds are noncritical and that there is zero force in the chord member.

From AISC *Manual* (AISC, 2017) Table 2-4, the material properties are as follows:

All members
ASTM A500 Grade C
F_y, $F_{yb} = 50$ ksi
F_u, $F_{ub} = 62$ ksi

From AISC *Manual* Table 1-11 and Table 1-12, the HSS geometric properties are as follows:

HSS 8×8×⅜
$A = 10.4$ in.^{2}
$B = 8.00$ in.
$H = 8.00$ in.
$t = 0.349$ in.

HSS 8×4×½
$A_b = 9.74$ in.^{2}
$B_b = 8.00$ in.
$H_b = 4.00$ in.
$t_b = 0.465$ in.

Solution:

Required strength (expressed as a force in the branch)

From ASCE/SEI 7 (ASCE, 2016) Chapter 2, the required strength of the connection is:

LRFD	ASD
$P_u = 1.2\ (50.0\text{ kips}) + 1.6\ (50.0\text{ kips})$ $= 140\text{ kips}$	$P_a = 50.0\text{ kips} + 50.0\text{ kips}$ $= 100\text{ kips}$

The strength of a matched-width ($\beta = 1.0$), welded, rectangular HSS to rectangular HSS cross-connection, under branch axial compression, can be determined from the limit states of web local yielding, web local crippling, and web compression buckling.

$$\beta = \frac{8.00\text{ in.}}{8.00\text{ in.}} = 1.00$$

Limit State of Web Local Yielding

From Equation 15 in Table 6,

$$P_n = 2F_y t\left(7.5t + \frac{H_b}{\sin\theta}\right) \tag{15}$$

$$= 2(50\text{ ksi})(0.349\text{ in.})\left[7.5(0.349\text{ in.}) + \frac{4.00\text{ in.}}{\sin 90^\circ}\right]$$

$$= 231\text{ kips}$$

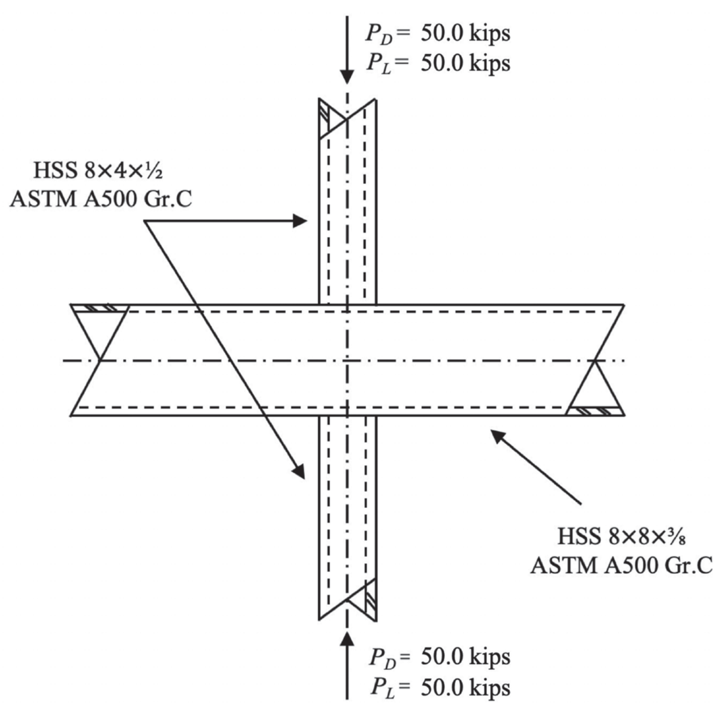

Fig. 12. Rectangular HSS-to-HSS cross-connection subjected to branch axial compression.

By applying the resistance factor of $\phi = 1.00$, and the safety factor of $\Omega = 1.50$, for this limit state (AISC *Specification* Section J10.2), the available strength (ϕP_n or P_n/Ω) is:

LRFD	ASD
$\phi P_n = 1.0(231 \text{ kips})$ $= 231 \text{ kips}$ $231 \text{ kips} > 140 \text{ kips}$ **o.k.**	$\dfrac{P_n}{\Omega} = \dfrac{231 \text{ kips}}{1.50}$ $= 154 \text{ kips}$ $154 \text{ kips} > 100 \text{ kips}$ **o.k.**

Limit State of Web Local Crippling

From Equation 16 in Table 6,

$$P_n = 1.6t^2 \left(1 + \frac{\dfrac{3H_b}{\sin\theta}}{H} \right) \sqrt{EF_y} Q_f \tag{16}$$

$Q_f = 1.0$ for a chord with no load, or a tension force, in accordance with AISC *Specification* Table K3.2.

$$\begin{aligned} P_n &= 1.6(0.349 \text{ in.})^2 \left[1 + \frac{\dfrac{3(4.00 \text{ in.})}{\sin 90^\circ}}{8.00 \text{ in.}} \right] \sqrt{(29{,}000 \text{ ksi})(50 \text{ ksi})}(1.0) \\ &= 587 \text{ kips} \end{aligned}$$

By applying the resistance factor of $\phi = 0.75$, and the safety factor of $\Omega = 2.00$, for this limit state (AISC *Specification* Section J10.3), the available strength is:

LRFD	ASD
$\phi P_n = 0.75(587 \text{ kips})$ $= 440 \text{ kips}$ $440 \text{ kips} > 140 \text{ kips}$ **o.k.**	$\dfrac{P_n}{\Omega} = \dfrac{587 \text{ kips}}{2.00}$ $= 294 \text{ kips}$ $294 \text{ kips} > 100 \text{ kips}$ **o.k.**

Limit State of Web Compression Buckling

$$H_b/\sin\theta = 4.00 \text{ in.} > 0.25H = 0.25(8.00 \text{ in.}) = 2.00 \text{ in.}$$

Hence, from Table 6, the member webs will be designed as compression members in accordance with AISC *Specification* Chapter E, using $K = 0.65$.

Critical Buckling Stress, F_{cr}

Calculate the effective slenderness ratio (L_c/r) using Equation 8, with $K = 0.65$, to determine applicable equation:

$$\frac{KL}{r} = \frac{L_c}{r} = 3.46K\left(\frac{H}{t} - 3\right)\sqrt{\frac{1}{\sin\theta}} \tag{8}$$

$$\begin{aligned} &= 3.46(0.65)\left(\frac{8.00 \text{ in.}}{0.349 \text{ in.}} - 3\right)\sqrt{\frac{1}{\sin 90^\circ}} \\ &= 44.8 \end{aligned}$$

$$4.71\sqrt{\frac{E}{F_y}} = 4.71\sqrt{\frac{29{,}000\text{ ksi}}{50\text{ ksi}}}$$
$$= 113.4$$

Because $\dfrac{KL}{r} < 4.71\sqrt{\dfrac{E}{F_y}}$, AISC *Specification* Equation E3-2 applies:

$$F_{cr} = \left(0.658^{\frac{F_y}{F_e}}\right)F_y \qquad \text{(\textit{Spec}. Eq. E3-2)}$$

where

$$F_e = \frac{\pi^2 E}{\left(\frac{L_c}{r}\right)^2}$$
$$= \frac{\pi^2(29{,}000\text{ ksi})}{(44.8)^2}$$
$$= 143\text{ ksi}$$

Hence,

$$F_{cr} = \left(0.658^{\frac{50\text{ ksi}}{143\text{ ksi}}}\right)(50\text{ ksi})$$
$$= 43.2\text{ ksi}$$

Flexural Buckling of the Chord Sidewalls

The nominal compressive strength of the two sidewalls, by flexural buckling, is given by AISC *Specification* Equation E3-1:

$$P_n = F_{cr}A_g \qquad \text{(\textit{Spec}. Eq. E3-1)}$$

where A_g for one sidewall is given by Equation 12. For two sidewalls,

$$A_g = 2\left(7.5t + \frac{H_b}{\sin\theta}\right)t \qquad (12)$$
$$= 2\left[7.5(0.349\text{ in.}) + \frac{4.00\text{ in.}}{\sin 90^\circ}\right](0.349\text{ in.})$$
$$= 4.61\text{ in.}^2$$

Therefore, the nominal strength of the two sidewalls in flexural buckling is:

$$P_n = (43.2\text{ ksi})(4.61\text{ in.}^2)$$
$$= 199\text{ kips}$$

By applying the resistance factor of $\phi_c = 0.90$, and the safety factor of $\Omega_c = 1.67$, for this limit state (AISC *Specification* Section E1), the available strength is:

LRFD	ASD
$\phi_c P_n = 0.90\,(199\text{ kips})$ $= 179\text{ kips}$ $179\text{ kips} > 140\text{ kips}$ **o.k.**	$\dfrac{P_n}{\Omega_c} = \dfrac{199\text{ kips}}{1.67}$ $= 119\text{ kips}$ $119\text{ kips} > 100\text{ kips}$ **o.k.**

As expected, because the bearing length is greater than $0.25H$, the connection resistance by web compression buckling governs. The connection shown in Figure 12 has an identical configuration to Specimen X2, which, as indicated in Table 5, failed by sidewall buckling.

ACKNOWLEDGMENTS

Financial support for this project was provided by the Natural Sciences and Engineering Research Council of Canada (NSERC). Hollow structural sections used for two experiments reported herein were donated by Atlas Tube, Harrow, Ontario.

SYMBOLS

A Cross-sectional area of rectangular HSS chord member, in.^{2}

A_b Cross-sectional area of rectangular HSS branch member, in.^{2}

A_g Cross-sectional area of element, in.^{2}

B Overall width of rectangular HSS chord member, perpendicular to the plane of the connection, in.

B_b Overall width of rectangular HSS branch member or plate, perpendicular to the plane of the connection, in.

COV Coefficient of variation

E Modulus of elasticity of HSS member, ksi

F_{cr} Critical stress of HSS chord member, ksi

F_u Ultimate tensile strength of HSS chord member, ksi

F_{ub} Ultimate tensile strength of branch member, ksi

F_y Yield stress of HSS chord member, ksi

F_{yb} Yield stress of branch member, ksi

F_{yw} Yield stress of web material, ksi

H Overall height of rectangular HSS chord member, perpendicular to the plane of the connection, in.

H_b Overall height of rectangular HSS branch member or plate, perpendicular to the plane of the connection, in.

K Effective length factor

L_c Effective length of member, in.

P Axial force, kips

P_D Axial force due to dead load, kips

P_L Axial force due to live load, kips

P_a Actual connection ultimate load, kips; required axial strength using ASD load combinations, kips

$P_{a,X1}$ Actual connection ultimate load of specimen X1, kips

$P_{a,X2}$ Actual connection ultimate load of specimen X2, kips

P_n Nominal connection strength, kips

P_u Required axial strength in tension or compression, using LRFD load combinations, kips

Q_f Chord-stress interaction parameter

R_n Nominal strength, kips

d Full nominal depth of member, in.

h Clear distance between flanges less the fillet or corner radius, in.

k Distance from outer face of flange to web toe of fillet for I-section, in.; outside corner radius for rectangular HSS section, in.

l_b Bearing length of the load, measured parallel to the axis of the HSS member, in.

l_{end} Distance from the near side of the connecting branch or plate to end of member, in.

t Wall thickness of rectangular HSS chord member, in.

t_b Wall thickness of rectangular HSS branch member, in.

t_f Thickness of flange, in.

t_w Thickness of web, in.

Ω Safety factor

β Ratio of branch width to chord width, perpendicular to the plane of the connection

χ Reduction factor for (column) buckling

ε_{rup} Strain at rupture

ε_y Strain at yield

τ Ratio of branch wall thickness to chord wall thickness

γ Chord slenderness; the ratio of one-half the width to wall thickness for rectangular HSS

η Load length parameter; the ratio of the length of contact of the branch with the chord in the plane of the connection to the chord width

ϕ Resistance factor

θ Acute angle between the branch and chord, degrees

REFERENCES

AISC (2010), ANSI/AISC 360-10, *Specification for Structural Steel Buildings*, American Institute of Steel Construction, Chicago, Ill.

AISC (2016), ANSI/AISC 360-16, *Specification for Structural Steel Buildings*, American Institute of Steel Construction, Chicago, Ill.

AISC (2017), *Steel Construction Manual*, 15th Ed., American Institute of Steel Construction, Chicago, Ill.

AISI (2016), AISI S100-16, *North American Specification for the Design of Cold-Formed Steel Structural Members*, American Iron and Steel Institute, Washington, D.C.

ASCE (2016), *Minimum Design Loads and Associated Criteria for Buildings and Other Structures*, ASCE/SEI 7-16, American Society of Civil Engineers, Reston, Va.

ASTM (2018), ASTM A500/A500M-18, *Standard Specification for Cold-Formed Welded and Seamless Carbon Steel Structural Tubing in Rounds and Shapes*, American Society for Testing and Materials, West Conshohocken, Pa.

CEN (2005), *Eurocode 3: Design of Steel Structures—Part 1-8: Design of Joints*, EN 1993-1-8:2005, European Committee for Standardization, Brussels, Belgium.

CSA (2013), CSA G40.20-13/G40.21-13, *General Requirements for Rolled or Welded Structural Quality Steel/Structural Quality Steel*, Canadian Standards Association, Toronto, Canada.

Davies, G. and Packer, J.A. (1987), "Analysis of Web Crippling in a Rectangular Hollow Section," *Proceedings of the Institution of Civil Engineers*, Part 2, Vol. 83, pp. 785–798.

Fisher, J.W., Ravindra, M.K., Kulak, G.L., and Galambos, T.V. (1978), "Load and Resistance Factor Design Criteria for Connectors," *Journal of the Structural Division,* ASCE*,* Vol. 104, No. 9, pp. 1,427–1,441.

IIW (2012), *Static Design Procedure for Welded Hollow Section Joints—Recommendations*, 3rd Ed., IIW Doc. XV-1402-12, International Institute of Welding, Paris, France.

ISO (2013), *Static Design Procedure for Welded Hollow Section Joints—Recommendations,* ISO 14346, International Organization for Standardization, Geneva, Switzerland.

Kuhn, J., Packer, J.A., and Fan, Y. (2019), "Rectangular Hollow Section Webs under Transverse Compression," *Canadian Journal of Civil Engineering*, Vol. 46, pp. 810–827.

Liu, J. (2016), "Updates to Expected Yield Stress and Tensile Strength Ratios for Determination of Expected Member Capacity in the 2016 AISC Seismic Provisions," *Engineering Journal,* AISC*,* Vol. 53, No. 4, pp. 215–227.

Lu, L.H., de Winkel, G.D., Yu, Y., and Wardenier, J. (1994), "Deformation Limit for the Ultimate Strength of Hollow Section Joints," *Sixth International Symposium on Tubular Structures*, Melbourne, Australia, pp. 341–347.

Newlin, D.E. and Chen, W.F. (1971), "Strength and Stability of Column Web in Welded Beam-to-Column Connections," Fritz Engineering Laboratory Report No. 333.14, Lehigh University, Bethlehem, Pa.

Packer, J.A. (1984), "Web Crippling of Rectangular Hollow Sections," *Journal of Structural Engineering*, ASCE, Vol. 110, No. 10, pp. 2,357–2,373.

Packer, J.A. (1987), "Review of American RHS Web Crippling Provisions," *Journal of Structural Engineering*, ASCE, Vol. 113, No. 12, pp. 2,508–2,513.

Packer, J.A., Wardenier, J., Zhao, X.-L., van der Vegte, G.J., and Kurobane, Y. (2009), *Design Guide for Rectangular Hollow Section (RHS) Joints under Predominantly Static Loading,* CIDECT Design Guide No. 3, 2nd Ed., CIDECT, Geneva, Switzerland.

Ravindra, M.K. and Galambos, T.V. (1978), "Load and Resistance Factor Design for Steel," *Journal of the Structural Division*, ASCE, Vol. 104, No. 9, pp. 1,337–1,353.

Roberts, T.M. (1981), “Slender Plate Girders subject to Edge Loading,” *Proceedings of the Institution of Civil Engineers*, Part 2, Vol. 71, No. 3, pp. 805–819.

Wei, F. (2019), “Experimental Study of Laterally Offset RHS X-Connections in Branch Axial Compression,” M.A.Sc. Thesis, University of Toronto, Toronto, Canada.